Enhanced azo dye (Sudan G) decolorization and simultaneous electricity generation using a bacterial consortium in a dual-chamber microbial fuel cell

Chinwendu Jude Echejiuba[1] , Chimezie Jason Ogugbue[1✉] and Ifeyinwa Sarah Obuekwe[2]

¹Department of Microbiology, Faculty of Science, University of Port Harcourt, Port Harcourt, Nigeria; ²Department of Microbiology, Faculty of Life Sciences, University of Benin, Benin City, Nigeria
✉**Corresponding author, E-mail:** *jason.ogugbue@uniport.edu.ng*

Abstract. Azo dyes are prevalent anthropogenic compounds, making their enhanced treatment crucial in our color-saturated world. This study examined the ability of a microbial consortium, comprising *Pseudomonas aeruginosa* (MW584979), *Enterobacter hormaechei* (MW584986), *Providencia stuartii* (MW584987), *Escherichia coli* (MZ394117), and *Pseudomonas xiamenensis* (MW585052), to decolorize Sudan orange G in a microbial fuel cell (MFC) after determining the optimal conditions for dye decoorization using response surface methodology (RSM) and the One Factor at a Time (OFAT) method. Degradation products were analyzed using the gas chromatography-mass spectroscopy technique. The consortium achieved an 88% decolorization rate within 24 hours under the optimal conditions identified by the Central Composite Design (CCD) of RSM. These conditions, pH 7.0, temperature 35, salinity 5 g/L, and glucose concentration 10 g/L, when applied in the MFC, resulted in an enhanced decolorization rate of 92% and simultaneous electricity generation of 130 mV within 24 hours. GC-MS analysis confirmed the breakdown of the azo dye into simpler, less toxic compounds. Metabolites produced through RSM and MFC processes were identified and compared with controls using chromatography-mass spectrometry. Degradation metabolites obtained after treatment of the dye wastewater in the MFC include Cyclopentane and cyclopropylidene-

2(1H)-naphthalenone which highlights the role of microbial enzymatic activity in converting complex azo dye structures into environmentally benign compounds. These results highlight the successful integration of RSM for process optimization and MFCs for enhanced biodegradation and renewable energy production. The scalability of this technique is promising, given the relatively simple and cost-effective setup of MFC systems. Moreover, the economic feasibility of large-scale deployment is enhanced by the dual benefits of wastewater treatment and renewable energy production, making it a sustainable solution for managing azo dye pollution.

Keywords: wastewater, biodegradation, 16srRNA, electricity generation, response surface methodology

Introduction

Synthetic dyes such as azo dyes have nitrogen-nitrogen double bond attached to the aromatic groups and are the main coloring agents in many industries including the textile industry (Cao *et al.*, 2019; Firoozeh *et al.*, 2022; Al-Tohamy *et al.*, 2023). They make up most of the synthetic dyes used in industries since they are easy to synthesize and cost effective however, some are carcinogenic and mutagenic and have been reported to be biotoxic (Das and Mishra, 2017; Chen *et al.*, 2021; Ngo and Tischler, 2022; Rafaqat *et al.,* 2022). Interestingly, about 10 to 15% of the synthetic dyes used in textile manufacturing are lost as wastewater effluent (Md *et al.*, 2021). Hence, treatment of synthetic textile wastewater is desirable. However, since physicochemical methods such as membrane filtration is energy and cost intensive, biotreatment using microorganisms is a safer, cost effective and ecofriendly way to tackle these wastewaters (Das and Mishra, 2017; Trivedi *et al.*, 2022; Al-Tohamy *et al.*, 2023). Trivedi *et al.* (2022) reported increase in azo dye methyl orange decolorization with increase in biomass concentration under denitrifying conditions.

Enacted strict laws and regulations have made the textile wastewater treatment an extensive research area worldwide (Al-Tohamy *et al.*, 2023), and bioremediation has been of great interest to researchers and industries, as the transition toward greener solutions has become more in demand in recent times (Cao *et al.*, 2019; Gul *et al.*, 2021; Ngo and Tischler, 2022; Al-Tohamy *et al.*, 2023). For example, indigenous microbial consortium obtained from a textile factory sedimentation tank enhanced the decolorization of an azo dye on a broad range of temperature, pH, salinity and dye concentrations (Cao *et al.*,

2019). Similarly, a halotolerant yeast consortium (*Sterigmatomyces halophilus* SSA-1575 and *Meyerozyma guilliermondii* SSA-1547) exhibited 96.1% decolorization efficiency when exposed to 50 mg/L of a reactive azo dye (Al-Tohamy *et al.*, 2023).

Microbial fuel cell (MFC) is an emerging and promising technology that addresses challenges of wastewater treatment while simultaneously incorporating bioelectricity production and CO2 emission reduction during microbial metabolism (Mittal and Kumar, 2022; Sikder and Rahman, 2023). This novel biological approach enhances the rate of anaerobic degradation of complex organics by introducing electrodes as an electron acceptor (Matteo, 2018). MFCs can enhance further the bioreduction of textile pollutants such as azo dyes as they have an infinite resource of terminal electron acceptors (anode) compared to exhaustible electron acceptors such as oxygen again, it has electricity generation as an additional advantage (Ilamathi and Jayapriya, 2017). Sikder and Rahman, (2023) demonstrated significant reduction in COD and TDS of municipal, textile and tannery wastewaters with better voltage and current generation from textile wastewater with MFC technology. Biodegradation of Remazol Brilliant Blue R (RBBR) was accompanied with electricity generation using fungal-based fuel cell (Umar *et al.*, 2023). Nk and Rahman, (2020) showed 77.03% COD removal with concomitant current production of 4.8 MA and power density of 16.8 mW/m^2 from textile wastewater using single chambered microbial fuel cell. Similarly, enhanced anaerobic treatment of dyeing wastewater with microbial fuel cell was most effective with electrode area ratio of 1:1 (Hu *et al.*, 2023).

The present study investigated the impact of different cultural conditions on the decolorization of an azo dye (Sudan G) with C.I. Number 11920 using five (5) azo dye degrading bacteria as well as MFC for enhanced decolorization.

Synthetic dyes, particularly azo dyes, are characterized by nitrogen-nitrogen double bonds attached to aromatic groups, and they serve as the primary coloring agents in various industries, including textiles (Cao *et al.*, 2019; Firoozeh *et al.*, 2022; Al-Tohamy *et al.*, 2023). These dyes dominate industrial applications due to their ease of synthesis and cost-effectiveness; however, many azo dyes are carcinogenic, mutagenic, and biotoxic, posing significant environmental and health risks (Das and Mishra, 2017; Chen *et al.*, 2021; Ngo and Tischler, 2022; Rafaqat *et al.*, 2022). Alarmingly, approximately 10 to 15% of synthetic dyes used in textile manufacturing are discharged as wastewater effluent, necessitating effective treatment strategies (Md *et al.*, 2021).

Traditional physicochemical methods for treating textile wastewater, such as membrane filtration, are often energy-intensive and expensive, making them less sustainable. In contrast, biotreatment using microorganisms offers a safer, cost-effective, and eco-friendly alternative to tackle these pollutants (Das

and Mishra, 2017; Trivedi *et al.*, 2022; Al-Tohamy *et al.*, 2023). For instance, Trivedi *et al.* (2022) reported enhanced decolorization of azo dye methyl orange with increasing biomass concentrations under denitrifying conditions. However, existing bioremediation techniques require optimization to address the limitations of efficiency and applicability across diverse environmental conditions.

Recent stringent laws and regulations governing textile wastewater discharge have driven extensive research into more sustainable and eco-friendly solutions (Al-Tohamy *et al.*, 2023). Among these, bioremediation has garnered significant interest due to its alignment with the global transition toward greener technologies (Cao *et al.*, 2019; Gul *et al.*, 2021; Ngo and Tischler, 2022). Microbial consortia derived from textile factory sedimentation tanks, for example, have demonstrated remarkable decolorization efficiencies for azo dyes under varying conditions of temperature, pH, salinity, and dye concentrations (Cao *et al.*, 2019). Similarly, halotolerant yeast consortia have achieved impressive decolorization rates of reactive azo dyes, emphasizing the potential of microbial approaches in treating dye-laden wastewaters (Al-Tohamy *et al.*, 2023).

However, despite the promise of bioremediation, the need for more efficient, scalable, and multifunctional systems has driven interest in microbial fuel cells. These systems combine wastewater treatment with the generation of bioelectricity and the reduction of CO_2 emissions during microbial metabolism, addressing environmental challenges on multiple fronts (Mittal and Kumar, 2022; Sikder and Rahman, 2023).

MFCs work by employing electrodes as terminal electron acceptors in microbial metabolism, enhancing the anaerobic degradation of complex organic pollutants such as azo dyes. Unlike traditional electron acceptors like oxygen, which are finite and location-dependent, the electrodes in MFCs provide a continuous and renewable alternative, supporting sustained microbial activity and degradation processes, as well as electricity generation (Ilamathi and Jayapriya, 2017; Matteo, 2018). This mechanism enables MFCs to significantly reduce chemical oxygen demand (COD) and total dissolved solids (TDS) in various types of wastewater, including municipal, textile, and tannery effluents. Notably, Sikder and Rahman (2023) observed superior voltage and current generation during the treatment of textile wastewater, highlighting the dual benefits of pollutant removal and energy production.

Furthermore, recent advances have demonstrated the potential for enhanced efficiency through system optimization. For instance, fungal-based MFCs successfully biodegraded Remazol Brilliant Blue R (RBBR) while generating electricity, showcasing the versatility of MFC technology (Umar *et al.*, 2023).

Similarly, Hu *et al.* (2023) reported improved anaerobic treatment of dyeing wastewater by optimizing the electrode area ratio, emphasizing both the adaptability and scalability of MFCs for industrial applications. This dual functionality not only addresses wastewater treatment challenges but also supports the transition toward green energy and reduction in carbon emissions. Moreover, the high scalability and adaptability potentials of MFC make them practical for industrial wastewater applications, where they can contribute to cost-effective, large-scale solutions with significant environmental and economic benefits.

This study builds on these advancements by investigating the impact of different cultural conditions on the decolorization of an azo dye (Sudan orange G) using a microbial consortium and exploiting MFC technology to enhance treatment efficiency and electricity generation, thereby addressing the dual objectives of effective azo dye degradation and renewable energy production. The findings aim to contribute to the growing body of research on sustainable solutions for managing industrial dye pollution.

Materials and methods

Textile wastewater and isolation of azo dye reducing bacteria

Sudan orange G, a dye routinely used by local dyers was used as the azo dye for the preparation of simulated textile wastewater in this study. High purity Sudan orange G dye was purchased from Aldrich Chemical Co, USA and was used without prior purification. The chemical structure of Sudan orange G is shown in Figure 1. The textile effluent used for bacterial isolation was kindly donated by Sunflag Nigeria Limited, and Kofar Mata Dye Pits. The textile effluent samples were enriched by introducing 10 mL of samples into 90 mL of mineral salt broth enhanced with 0.01% of Sudan orange G dye and contained in 250 mL Erlenmeyer flask. Serial dilutions were made from the enriched culture of the textile effluent up to dilution 10^{-3}. Subsequently, mineral salt agar medium enhanced with 0.01% of Sudan orange G dye was inoculated with 0.1 mL of each suspension, spread with a glass spreader and incubated at 37 for 72 hrs. After incubation, zone of clearance around distinct colonies was taken as evidence of decolorization and organisms exhibiting dye decolorization potential were identified. The same medium was inoculated with a suspension derived from a stream water sample, which served as the control. No zones of clearing were observed on the control plates.
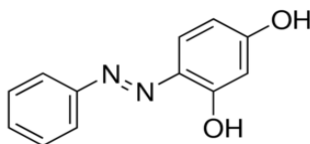
Figure 1. Chemical structure of Sudan orange G

Bacterial community identification

Identification of bacterial isolates were based on molecular technique and characterization using Polymerase chain reaction (PCR) with appropriate primers at Molecular Biology Unit, Medical laboratory Science Department, Niger Delta University (Bayelsa State).

DNA extraction. Five milliliters (5 mL) of an overnight broth culture of the bacterial isolate in Luria Bertani (LB) medium was spun at 14, 000 rpm for 3 mins. The cells were re-suspended in 500 µL of normal saline and heated at 95°C for 20 mins. The heated bacterial suspension was cooled on ice and spun for 3 mins at 14, 000 rpm. The supernatant containing the DNA was transferred to a 1.5 mL microcentrifuge tube and stored at -20℃ for other downstream reactions. or Gram-positive bacteria with tougher cell walls, the boiling method was supplemented with additional steps to enhance lysis and improve DNA yield. One such step involved treating the bacterial cells with lysozyme, facilitating more effective DNA extraction.

DNA quantification. The extracted genomic DNA was quantified using the Nanodrop 1000 spectrophotometer. DNA purity was assessed by measuring the A260/A280 ratio, which provides an indication of protein contamination. A ratio within the range of 1.8–2.0 was considered acceptable, ensuring the DNA was of sufficient quality for downstream applications such as PCR amplification and sequencing.

The software of the equipment was launched by double clicking on the Nanodrop icon. The equipment was initialized with 2 µL of sterile distilled water and blanked using normal saline. Two microliters (2 µL) of the extracted DNA were loaded onto the lower pedestal; the upper pedestal was brought down to contact the extracted DNA on the lower pedestal. The DNA concentration was measured by clicking on the "measure" button.

16S rRNA amplification. The 16s rRNA region of the rRNA gene of the isolates were amplified using the 27F: 5'-AGAGTTTGATCMTGGCTCAG-3' and 1492R: 5'-CGGTTACCTTGTTACGACTT-3' primers on an ABI 9700 Applied Biosystems thermal cycler at a final volume of 40 microlitres for 35 cycles.

The PCR mix utilized for amplification included the X2 Dream Taq Master Mix supplied by Inqaba, South Africa, which contains Taq polymerase, dNTPs, and MgCl$_2$ at optimized concentrations suitable for standard PCR reactions. The final concentration of primers in the reaction was 0.5 µM, and the total reaction volume was 40 µL. While the precise concentrations of Taq polymerase, dNTPs, and MgCl$_2$ are proprietary to the master mix formulation, these are pre-optimized by the manufacturer to ensure reproducibility and efficient amplification. The PCR conditions were as follows: Initial denaturation, 95℃ for 5 minutes; denaturation, 95℃ for 30 seconds; annealing, 52℃ for 30 seconds; extension, 72℃ for 30 seconds for 35 cycles and final extension, 72℃ for 5 mins. The product was resolved on a 1% agarose gel at 130 V for 30 mins and visualized on a blue light transilluminator.

Sequencing. Sequencing was done using the BigDye Terminator kit on a 3510 ABI sequencer by Inqaba Biotechnological, Pretoria South Africa. The sequencing was done at a final volume of 10 µL; the components included 0.25 µL BigDye® terminator v1.1/v3.1, 2.25 µL of 5 x BigDye sequencing buffer, 10 µM Primer PCR primer, and 2-10 µg PCR template per 100 bp. The sequencing condition were as follows; 32 cycles of 96 for 10s, 55 for 5s and 60 for 4 mins. Sequencing quality was assessed by reviewing chromatograms generated from the 3510 ABI sequencer using appropriate sequencing analysis software. Key metrics, such as the quality scores (Phred scores) and the clarity of the chromatogram peaks, were evaluated to ensure high-quality reads. Any low-quality sequences or ambiguous base calls were addressed by trimming the affected regions using sequence editing software such as BioEdit or MEGA. If significant issues persisted, such as incomplete reads or unclear chromatograms, re-sequencing was performed to obtain accurate data. These steps ensured the reliability of the sequences used for subsequent phylogenetic analysis.

Phylogenetic analysis. The obtained sequences were edited using the Trace Edit bioinformatics algorithm to ensure accuracy. Similar sequences were retrieved from the National Center for Biotechnology Information (NCBI) database using BLASTN. The BLAST search parameters included default settings for gap penalties and scoring, with the top hits selected based on sequence identity (≥97%), query coverage, and relevance to taxonomy. Only closely related sequences with high identity scores were chosen for downstream analysis. Sequences were aligned using the MAFFT software with default settings to ensure accurate multiple sequence alignment. The evolutionary history was inferred using the Neighbor-Joining method in MEGA 6.0, employing the Jukes-Cantor model for sequence evolution. The reliability of the phylogenetic tree was assessed through bootstrap analysis with 500 replicates, and bootstrap values were included to validate the confidence of the tree branches.

The sequences obtained in this study were submitted to the GenBank database and assigned the following accession numbers: *Pseudomonas aeruginosa* (MW584979), *Enterobacter hormaechei* (MW584986), *Providencia stuartii* (MW584987), *Escherichia coli* (MZ394117), and *Pseudomonas xiamenensis* (MW585052). This ensures transparency and facilitates accessibility for future research. The decolorization abilities of the bacterial isolates were evaluated using Sudan orange G and maintained in Bushnell Haas broth at 37 for routine experiments.

Azoreductase (azR) gene amplification

The azR gene of the isolates was amplified using the primers azRF (5'-GCGGATG(GC)G(GA)TTGTATTAT-3') and azRR (5'-ATCAAGCAC(AC)A(CG)(TC)TG(CT)TT-3') on an ABI 9700 Applied Biosystems thermal cycler in a 40 µL reaction volume for 35 cycles. These primers were sourced from literature and validated for specificity through initial PCR trials to ensure reliable amplification of the target gene in the bacterial species studied.

The PCR mix contained Taq polymerase for 5 minutes, followed by 35 cycles of denaturation at 95℃ for 30 seconds, annealing at 57℃ for 30 seconds, and extension at 72℃ for 30 seconds. A final extension step was performed at 72℃ for 5 minutes.

The PCR products were resolved on a 1% agarose gel, which was run at 130 V for 30 minutes. A DNA ladder was included on the gel to determine the molecular sizes of the PCR products. The gel was stained with SYBR Green, and the bands were visualized using a blue light transilluminator. These steps ensured the successful amplification and confirmation of the azR gene for further analysis

Effect of cultural conditions on biodecolorization

The medium here contained mineral salt broth (10 mL) inoculated with 10 mL of azo dye reducing bacteria at 0.5 McFarland standard solution homogeneity of each of the bacterial species (*Pseudomonas aeruginosa* (MW584979), *Enterobacter hormaechei* (MW584986), *Providencia stuartii* (MW584987), *Escherichia coli* (MZ394117) and *Pseudomonas xiamenensis* (MW585052) with 0.1 cc g/L of the dye for 24 hrs. The 0.5 McFarland standard was chosen as it provides a consistent measure of bacterial density, approximately equivalent to 1.5×10^8 CFU/mL, which is commonly used in microbial assays for ensuring uniform inoculum size. It served as a general benchmark for the initial inoculum, ensuring comparable starting conditions for all isolates. Thereafter, microbial growth and decolorization were based on UV-visible light spectrophotometer (LaMotte Smart) at 600 nm and 388 nm respectively.

Effect of pH. The effect of pH on dye decolorization by bacterial isolates was determined using different regimes of pH (4, 5, 6, 7, 8, 9 and 10). The pH of the medium was adjusted using 1N solutions of HCl and NaOH to achieve the desired pH values (4, 5, 6, 7, 8, 9, and 10) before inoculation. Sets of Erlenmeyer flasks containing 20 mL each of mineral salt broth containing 0.1 g/L dye were prepared and inoculated with 10 mL of the respective bacterial isolates and incubated at 35 for 24 hrs. No inoculum was added in the control tube. Thereafter, the extent of decolorization in each flask was assessed by centrifuging each broth culture samples at 12,000 rpm for 15 mins after which the supernatant was analyzed using a UV-visible light spectrophotometer (Chen *et al.,*2003). During the experiment, the pH was not actively monitored or readjusted, as the focus was on assessing the initial pH's impact on dye decolorization.

Effect of temperature. Mineral salt broth (20 mL) containing 0.1 g/L dye was inoculated with 10 mL of the respective bacterial isolates at different temperatures (15, 20, 25, 30, 35, 40 and 45℃) and incubated for 24 hrs. The temperature of the incubation was controlled using thermostatically regulated incubators set to the desired temperatures. Each incubator was pre-calibrated to ensure accuracy, and the temperature was monitored periodically during the 24-hour incubation period using a thermometer placed inside the incubator. This ensured consistent temperature conditions throughout the experiment for all bacterial isolates. No inoculum was added in the control tube and dye concentration was same in all tubes. Thereafter, the extent of decolorization in each flask was assessed by centrifuging each broth culture samples at 12,000 rpm for 15 mins after which the supernatant was analyzed using a UV-visible light spectrophotometer (Chen *et al.,*2003).

Effect of glucose. To evaluate the effect of glucose concentration on microbial dye decolorization, different concentrations of glucose ranging from 0.1 g/L to 10 g/L were prepared in mineral salt broth, each containing 0.1 g/L of the dye. These glucose concentrations were selected based on prior experiments to assess the impact of carbon source availability on microbial activity, including dye decolorization.

A 20 mL volume of each glucose concentration was dispensed into Erlenmeyer flasks and sterilized by autoclaving. After sterilization, 10 mL of an 18-hour old microbial culture was added to each flask, and the flasks were incubated at 35 for 24 hours. Control tubes, in which no inoculum was added, were included to ensure that the dye concentration remained constant across all treatments. After the incubation period, the tubes were centrifuged at 12,000 rpm for 15 minutes to separate the cells from the supernatant.

The supernatants were then analyzed spectrophotometrically to determine the extent of dye decolorization. Dye reduction was measured by comparing the absorbance of the supernatants at the appropriate wavelength before and after the incubation period.

Effect of different sodium salts. Sodium chloride and sodium citrate were used at different concentrations (0-10 g/L) to determine their effect on dye decolorization. High sodium chloride levels can inhibit bacterial growth in non-halotolerant species, negatively impacting decolorization whereas, sodium citrate may enhance dye decolorization by chelating metal ions that inhibit enzymatic activity. Mineral salts broth (20 mL) containing dye concentration (0.1 g/L) and different concentrations (0 – 10 g/L) of sodium chloride and sodium citrate each was inoculated with 10 mL of the respective bacterial isolate and incubated at 35°C for 24 hrs. Thereafter, the extent of decolorization in each flask was assessed by centrifuging each broth culture sample at 12,000 rpm for 15 mins after which the supernatant was analyzed using a UV-visible light spectrophotometer (Chen *et al.,*2003).

Effects of nitrogen sources. The effect of various nitrogen sources on dye decolorization by bacterial isolates was determined using urea and peptone as nitrogen sources. Urea and peptone were selected as nitrogen sources for this study due to their widespread use in microbial growth media and their ability to provide essential nitrogen for bacterial metabolism. Urea serves as a simple, inorganic nitrogen source, while peptone is a complex organic nitrogen source rich in amino acids and peptides. These distinct properties allow for the assessment of how different forms of nitrogen influence bacterial dye decolorization efficiency. Sets of Erlenmeyer flasks containing 70 mL each of sterile mineral salt broth containing 0.1g/L dye and 20 mL of different concentration (0 g/L to 10 g/L) of sterile urea or peptone were prepared and inoculated with 10 mL of the respective bacterial isolates. The chosen concentration range (0 g/L to 10 g/L) reflects conditions that encompass both nitrogen-limited and nitrogen-rich environments, ensuring a comprehensive evaluation of the bacterial isolates' response under varying nitrogen availability. After inoculation, the flasks were incubated at 35℃ for 24 hrs. Thereafter, the extent of decolorization in each flask was assessed by centrifuging each broth culture sample at 12,000 rpm for 15 mins after which the supernatant was analyzed using a UV-visible light spectrophotometer (Chen *et al.,* 2003).

Effect of vitamins. Vitamins B_2 and B_{12} were used at different concentrations (0–10 g/L) to determine their effect on dye decolorization efficiency, thereby contributing to the optimization of bioremediation strategies. Vitamin B2 (riboflavin)

and vitamin B12 (cobalamin) were selected for this study due to their critical roles in microbial metabolism and enzymatic functions. vitamin B2 is a precursor for flavin adenine dinucleotide (FAD) and flavin mononucleotide (FMN), which are cofactors involved in various redox reactions essential for microbial energy production and enzymatic activities. Similarly, vitamin B12 is a cofactor for enzymes that facilitate key metabolic processes, such as methylation and reductive reactions, which may directly or indirectly influence the decolorization of dyes by supporting the enzymatic pathways responsible for breaking down azo bonds. The concentration range tested was selected based on preliminary experiments, ensuring that the concentrations covered a spectrum of physiological relevance without causing vitamin-induced toxicity or metabolic imbalance.

Mineral salts broth (20 mL) containing these different vitamin concentrations was each inoculated with 10 mL of the respective bacterial isolate and incubated at 35℃ for 24 hrs. Thereafter, the extent of decolorization in each flask was assessed by centrifuging each broth culture sample at 12,000 rpm for 15 mins after which the supernatant was analyzed using a UV-visible light spectrophotometer (Chen *et al.,* 2003).

Optimization of dye decolorization using response surface methodology

The central composite design of the response surface methodology (Design Expert-13) was used to optimize the decolorization of the dyes using the values in (Table 1) below. Response surface methodology (RSM) is an approach used to generate the best conditions for a system comprising many variables to calculate the combined effect of selected variables. In the present study, RSM was employed to identify the interaction between the operational variables such as pH, temperature, glucose concentration and salinity using the central composite design (Table 2).

Table 1. Range and levels of experimental variables
for decolorization of Sudan orange G by consortium

| Factors	Levels				
	-α	-1	0	+1	+ α
pH	5	6	7	8	9
Temperature (°C)	25	30	35	40	45
Glucose concentration	0.5	0.75	1	1.25	1.5
Salinity	1	3	5	7	9

Table 2. The number of runs and factors sed
for the central composite design experiment

Std	Run	Factor 1 A: pH	Factor 2 B: Temp. (°C)	Factor 3 C; Glucose Conc. (g/L)	Factor 4 D: Salinity (%)	Response 1 % Decolorization	Response 2 Microbial Growth (600 nm)
22	1	7	35	14	5	62.65	1.42
19	2	7	25	10	5	44.02	0.38
6	3	8	30	12	3	51.02	0.53
2	4	8	30	8	3	54.12	0.69
25	5	7	35	10	5	74.14	1.78
16	6	8	40	12	7	56.74	0.76
9	7	6	30	8	7	52.81	0.62
12	8	8	40	8	7	54.89	0.73
15	9	6	40	12	7	68.25	1.61
14	10	8	30	12	7	60.86	0.98
17	11	5	35	10	5	61.02	1.09
1	12	6	30	8	3	54.78	0.71
27	13	7	35	10	5	81.73	2.12
8	14	8	40	12	3	70.12	1.73
18	15	9	35	10	5	69.18	1.71
13	16	6	30	12	7	62.74	1.48
21	17	7	35	6	5	62.64	1.38
26	18	7	35	10	5	75.47	1.89
20	19	7	45	10	5	39.87	0.34
4	20	8	40	8	3	67.85	1.58
5	21	6	30	12	3	51.81	0.58
11	22	6	40	8	7	48.89	0.48
23	23	7	35	10	1	47.28	0.43
3	24	6	40	8	3	58.98	0.89
10	25	8	30	8	7	51.02	0.53
7	26	6	40	12	3	57.87	0.83
24	27	7	35	10	9	68.81	1.64

Microbial fuel cell setup

A double chambered microbial fuel cell was used for enhanced decolorization of the dye (Sudan orange G). The set up comprised 0.1 g/L of the dye in 500 mL nutrient broth, two graphite rod electrodes (7.0 x 56.0 mm), copper wire conductor (1 mm diameter), multimeter and 2500 mL containers. The anode chamber of the MFC consisted of poultry dung mixed with sterile water to obtain a semi solid consistency. Poultry dung was used as the anode substrate

in this MFC setup due to its high organic matter content and diverse microbial population, which can facilitate the breakdown of organic compounds and generate electrons through microbial metabolism. The cathode chamber consisted of the dye inoculated with 1 mL of azo dye reducing bacteria at 0.5 McFarland standard solution homogeneity (*Pseudomonas aeruginosa* (MW584979), *Enterobacter hormaechei* (MW584986), *Providencia stuartii (*MW584987), *Escherichia coli* (MZ394117) and *Pseudomonas xiamenensis* (MW585052). Before use in the MFC, the electrodes were polished with fine sandpaper or abrasive material to remove surface oxidations and increase surface area for enhanced microbial attachment and electron transfer. The graphite rod electrodes were then carefully prepared to prevent contamination and ensure optimal performance. This preparation typically involves cleaning the electrodes with ethanol to remove oils or impurities, followed by rinsing them with distilled water. Both chambers were connected using a salt bridge (3 cm length; 1cm diameter) loaded with saline molten agar prepared by adding 10 g of sodium chloride in 100 mL of sterile water. Generation of electric current in the MFC was determined using a multimeter connected to the two graphite rods in each chamber via copper wire. Power (mv) produced were obtained at intervals of 12 hours for 3 days. Optimal conditions (as determined by RSM) were maintained in the cathode chamber during the experiment.
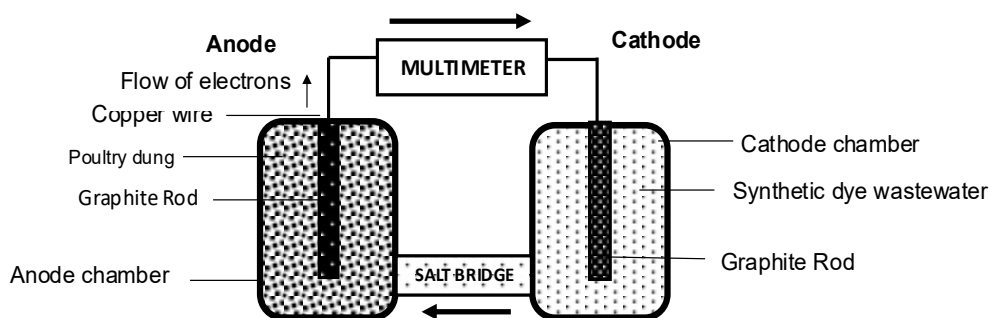
Figure 2. The microbial fuel cell

Bio decolorization, biodegradation and chemical analysis

Sudan orange G colour removal was monitored every 12 h using UV-visible light spectrophotometer at the maximum absorbance wavelength (λmax) of dye (i.e., 388 nm). Dye biodegradation was monitored by gas-chromatography-mass spectrometry (GC-MS). After dye degradation (3 days), the samples were centrifuged at 12,000 rpm for 5 min and the supernatants obtained were used

to extract metabolites. Thereafter, the absorbance of Sudan orange G broth was monitored in a UV-visible spectrophotometer at maximum absorption wavelength (388 nm). All the experiments were performed in triplicate and the results were expressed in terms of percentage decolorization as calculated using the formula (Eq.1) (Uppala *et al.*, 2015).

$$\textbf{Eq. 1. } Decolorization \% = \frac{Initial\ Absorbance - Final\ Absorbance}{Initial\ Absorbance} \times 100$$

The chemical changes in the redox dyes during decolorization were analyzed using Gas Chromatography-Mass Spectrometry (GC-MS). For sample preparation, an aliquot of the decolorized dye was transferred into Erlenmeyer flasks, and 15 mL of methanol was added. The mixture was vigorously agitated and left to stand for 24 hours. Following this, the extract was filtered through No.1 Whatman filter paper using a funnel, and the filtrate was collected in a 100 mL conical flask. The resulting extract was then subjected to GC-MS analysis.

One microliter (1 µL) of the methanol extract was injected into the GC-MS instrument. The GC oven temperature program was as follows: an initial temperature of 60 for 2 minutes, followed by a ramp to 300 at a rate of 10 per minute, and held at 300 for 6 minutes. The mass spectrometer was operated with a transfer line temperature of 240, ion source temperature of 240, and an electron ionization energy of 70 eV. The scan interval was set at 0.1 seconds, with a scan time of 0.2 seconds, and a scan range from 50 to 600 Daltons. The GC-MS method was validated by assessing specificity, precision, and accuracy using standard reference compounds. The spectra obtained from the GC-MS were processed using TurboMass Ver 5.4.2 software and compared to the National Institute of Standards and Technology (NIST-2008) standard library database for compound identification.

Results and Discussion

The 16S rRNA sequence obtained from the isolate showed a 100% similarity with sequences in the NCBI non-redundant nucleotide (nr/nt) database, matching species such as *Providencia stuartii*, *Pseudomonas aeruginosa*, *Pseudomonas xiamenensis*, *Escherichia coli*, and *Enterobacter hormaechei*. Phylogenetic analysis using the Jukes-Cantor method revealed that the isolates are closely related to these species, with evolutionary distances supporting their placement within the genera *Providencia*, *Pseudomonas*, *Escherichia*, and *Enterobacter*. The sequences and their respective accession numbers were as follows: *Pseudomonas aeruginosa* (MW584979), *Enterobacter hormaechei* (MW584986),

Providencia stuartii (MW584987), *Escherichia coli* (MZ394117), and *Pseudomonas xiamenensis* (MW585052) (Table 2). This genetic analysis confirms the close evolutionary relationships of the isolates with these species, as shown in (Figure 3) and (Figure 4).
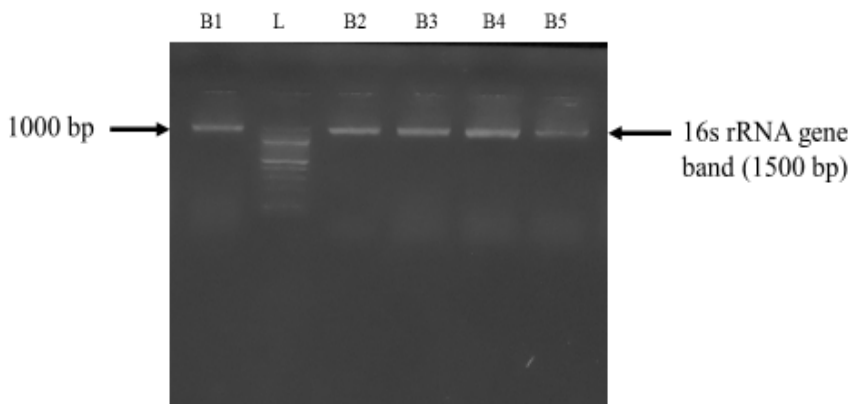
Figure 3. Agarose gel electrophoresis of the 16S rRNA gene of some selected bacterial isolates. Lanes B1-B5 represent the 16SrRNA gene bands (1500bp), lane L represents the 100bp molecular ladder. Key: B1= *Pseudomonas aeruginosa*; B2= *Enterobacter hormaechei*; B3= *Providencia stuartii*; B4= *Escherichia coli*; B5= *Pseudomonas xiamenensis.*
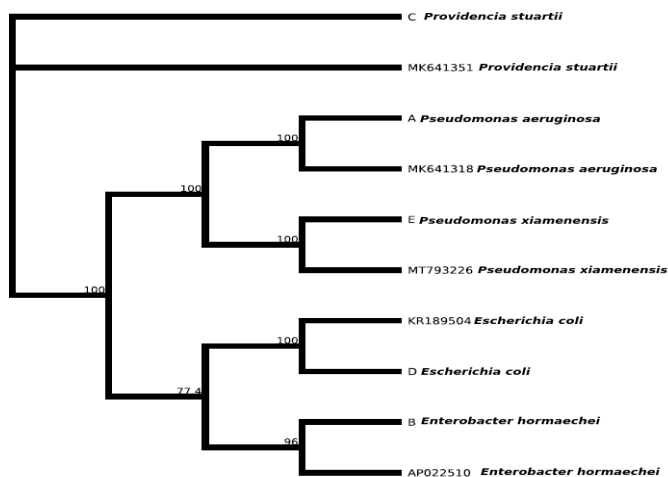

Figure 4. Neighbor-Joining tree based on 16S RNA gene sequence showing Relationship between *Providencia startii, Pseudomonas aeruginosa, Pseudomonas xiamenensis, Escherichia coli,* and *Enterobacter hormaechei.* Key: A= *Pseudomonas aeruginosa;* B= *Enterobacter hormaechei;* C= *Providencia stuartii;* D= *Escherichia coli;* E= *Pseudomonas xiamenensis*

The sequences obtained and their corresponding accession numbers were: *Pseudomonas aeruginosa* (MW584979), *Enterobacter hormaechei* (MW584986), *Providencia stuartii* (MW584987), *Escherichia coli* (MZ394117), and *Pseudomonas xiamenensis* (MW585052) (Table 2). This data provides a detailed genetic characterization, confirming the high similarity and close evolutionary relationships of the isolates with these known bacterial species. (Figure 5) depicts the agarose gel electrophoresis of the *azR* gene. Lanes A and C represent the *azR* at 500bp while lane L represents the 100 bp molecular ladder affirming that some of the bacterial species (*Pseudomonas aeruginosa* and *Providencia stuartii*) possess the azoreductase enzyme gene in their chromosomes.

Table 3. Accession numbers of bacteria isolated from textile waste water

Isolate Code	Accession Number	Similarity Index (%)	Bacterial Species
A	MW584979	100	*Pseudomonas aeruginosa*
B	MW584986	96	*Enterobacter hormaechei*
C	MW584987	100	*Providencia stuartii*
D	MZ394117	100	*Escherichia coli*
E	MW585052	100	*Pseudomonas xiamenensis*
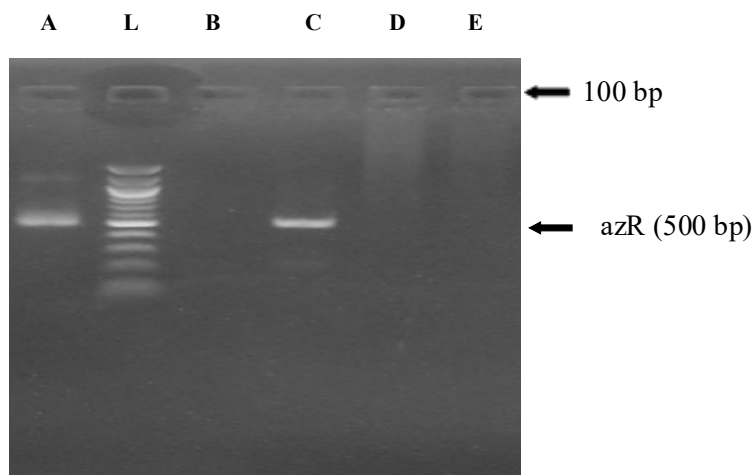
Figure 5. Agarose gel electrophoresis of the azR gene. Lanes A and C represent the azR at 500bp while lane L represents the 100 bp molecular ladder.Key: A= *Pseudomonas aeruginosa;* B= *Enterobacter hormaechei;* C= *Providencia stuartii;* D= *Escherichia coli;* E= *Pseudomonas xiamenensis*

Azoreductases play a crucial role in the bacterial degradation of azo dyes, a major class of synthetic dyes widely used in various industries. Azo dyes are characterized by the presence of one or more azo linkages (-N=N-). The *azr* gene encodes azoreductase enzymes, which catalyze the reductive cleavage of these azo bonds. This cleavage is a critical initial step in the biodegradation pathway of azo dyes, breaking down the complex dye molecule into smaller, less colored, and potentially less toxic aromatic amines. The general biochemical pathway involves the transfer of electrons from NADH or NADPH to the azo bond, resulting in its cleavage. This reaction typically occurs under anaerobic or microaerobic conditions.

The *azr* gene was chosen for investigation because azoreductase activity is a key indicator of a bacterium's ability to decolorize azo dyes. Detecting the presence of the *azr* gene provides direct evidence of the potential for azo dye degradation. Furthermore, the *azr* gene is a commonly studied marker in research on bacterial dye decolorization, allowing for comparisons with other studies.

The detection of the *azr* gene in *Pseudomonas aeruginosa* and *Providencia stuartii* in this study is consistent with previous research. Azoreductase activity has been widely reported in various bacterial species such as *Shewanella oneidensis*, *Rhodococcus opacus*, *Halomonas elongata*, and *Pseudomonas putida* (Qi *et al.*, 2016; Mendes *et al.*, 2011; Mugerfeld *et al.*, 2009; Qi *et al.*, 2017; Eslami *et al.*, 2016).

The data on the effect of various pH levels on dye decolorization by isolates, as presented in (Figure 6), reveal critical insights into the process's sensitivity to this environmental factor. Optimal decolorization for both dyes was achieved at a neutral pH of 7. This suggests that the enzymes or other biological mechanisms responsible for dye breakdown within the bacterial isolates function most efficiently under these conditions. As the pH shifted towards acidity (pH 4), the decolorization efficiency significantly declined, with the lowest performance observed at this most acidic level. Similarly, as the pH increased towards alkalinity, the decolorization extent also decreased. These trends are consistently illustrated in Figure 4 for all dyes tested. The significant differences ($p < 0.05$) in the percentage of dye decolorization at various pH levels underscore the pronounced impact of pH on the decolorization process.

The strong pH dependence observed can be attributed to several factors. Firstly, pH significantly influences the activity and stability of enzymes. Many enzymes have specific pH optima, and deviations from this optimum can lead to conformational changes that reduce or abolish their catalytic activity. The enzymes involved in dye degradation within the bacterial isolates likely exhibit such pH sensitivity. Secondly, pH affects the surface charge of both the bacterial cells and the dye molecules. At extreme pH values, the charges on the bacterial

cell surface and the dye molecules might become similar, leading to electrostatic repulsion and hindering the interaction between the bacteria and the dye. This reduced interaction can limit dye adsorption onto the bacterial cells, a crucial initial step in the decolorization process. Thirdly, pH can impact the redox potential of the system, influencing the availability of electron donors and acceptors needed for enzymatic reactions involved in dye breakdown.
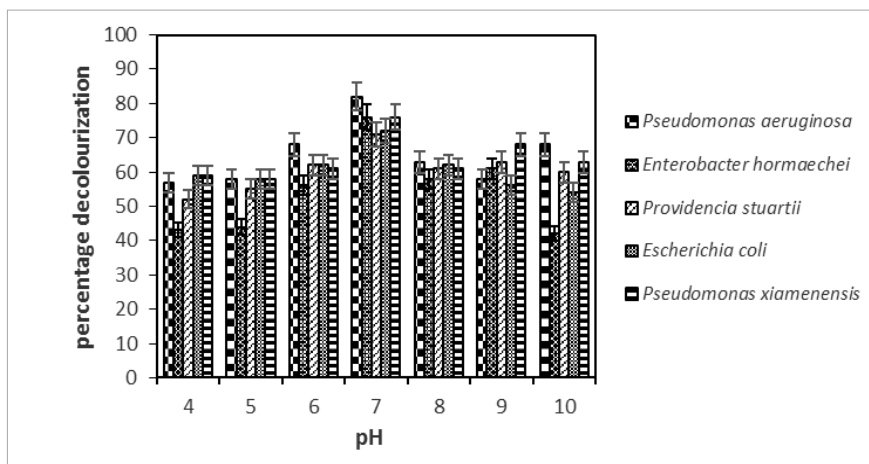

Figure 6. Effect of various pH on decolorization extent of Sudan orange G

These results are consistent with findings reported in the literature for other dye-decolorizing bacteria. For instance, studies on degradation of Malachite green by a bacterial culture have also demonstrated optimal dye decolorization at neutral or near-neutral pH, with decreased efficiency at both acidic and alkaline pH values (Etezad and Sadeghi-Kiakhani, 2021). Similarly, research on decolorization of Orange II by *Bacillus subtilis* has shown that pH affects the expression of dye-degrading enzymes, with optimal expression often observed around neutral pH (Ikram *et al.*, 2022). The near-neutral pH range also aligns with the findings of Liu *et al.* (2017), who suggested that slightly acidic to neutral pH is generally optimal for bacterial dye degradation, although the specific range can vary depending on the microbial consortium. Deviations from this range can affect enzyme structure and activity, thus reducing decolorization efficiency, as well as impacting microbial growth and community dynamics, as highlighted by Lui *et al.* (2016).

However, it's important to note that the specific pH optima and the extent of pH influence can vary depending on the bacterial species, the type of dye, and the specific enzymatic mechanisms involved. For example, Methyl orange

decolorization has been shown to be optimal under slightly alkaline conditions (Trivedi *et al*., 2022), whereas Mordant Black 11 dye removal by *Staphylococcus* sp. MB377 is favored by acidic pH (Tahir *et al*., 2021). This variability highlights the importance of characterizing the pH dependence of dye decolorization for each specific bacterial isolate and dye combination.

The impact of various temperature regimes on dye decolorization by different bacterial isolates is illustrated in (Figure 7). The data clearly demonstrate that the highest level of dye decolorization was achieved at an optimal temperature of 35℃, highlighting the enhanced metabolic activity and efficiency of the isolates at this temperature. This optimal temperature suggests that the enzymes involved in the dye degradation pathways within these bacteria are most efficient around 35℃. Enzymes, being biological catalysts, typically have a temperature range within which they function optimally. Beyond this range, their activity can decrease due to denaturation or other conformational changes.
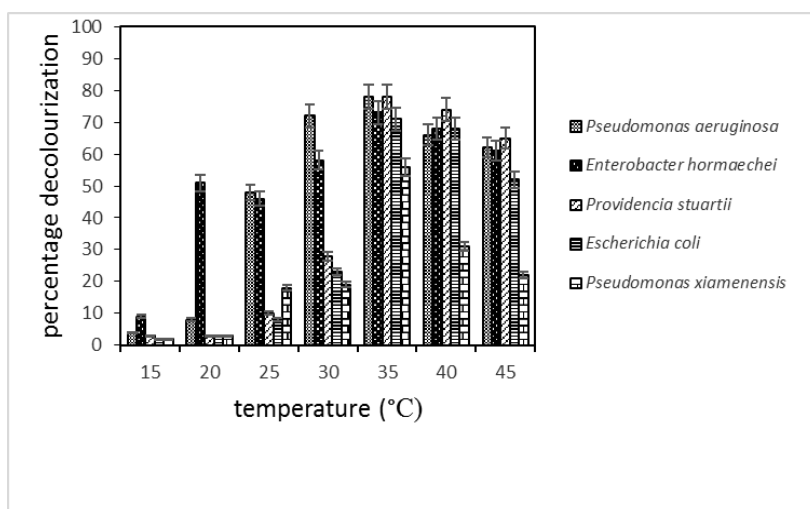
Figure 7. Effect of different temperature regimes
on decolorization extent of Sudan orange G

Conversely, the lowest decolorization performance was recorded at 15, indicating that lower temperatures significantly impede the decolorization process. At lower temperatures, the metabolic activity of the bacteria slows down. This includes reduced enzyme activity, slower transport of molecules across cell membranes, and decreased rates of biochemical reactions essential for dye degradation. Essentially, the bacteria are less metabolically active and therefore less efficient at breaking down the dye molecules.

These findings underscore the importance of maintaining an optimal temperature to maximize the efficacy of bacterial dye decolorization, providing a direction for the development and optimization of bioremediation protocols. The 35 optimum observed in this study is consistent with the typical growth temperature range for many mesophilic bacteria, which thrive in moderate temperatures (20-45). Many studies have reported similar optimal temperatures for dye decolorization by various bacterial species. For example, in a study by Ikram *et al.* (2022) it was shown that optimal dye removal was at 35 during decolorization of Orange II by *Bacillus subtilis*. Similarly, a bacterium has also demonstrated enhanced Malachite green decolorization at temperatures close to 35 (Etezad and Sadeghi-Kiakhani, 2021). Dafale *et al.* (2016) also reported the moderate temperature range (25 to 35) as optimal for bacterial dye degradation. Taha *et al.* (2014) emphasized the importance of temperature control for optimizing microbial activity and minimizing the release of harmful intermediates during dye degradation.

However, it's important to note that the optimal temperature for dye decolorization can vary depending on the specific bacterial species, the type of dye, and other environmental factors. Some bacteria, such as *Proteus mirabilis*, can thrive and degrade pollutants at higher temperatures of 40 (Madhushika *et al.*, 2021). Therefore, while 35 appears to be optimal for the isolates in this study, it's not a universal optimum for all dye-decolorizing bacteria.

The results on the effects of glucose concentration on dye decolorization by various bacterial Isolates are detailed in (Figure 8). The data reveal that the optimal decolorization of dyes was achieved at a glucose concentration of 10 g/L, showcasing the most efficient breakdown and removal of dye compounds under these conditions. In contrast, the lowest decolorization performance was observed at a glucose concentration of 0.1 g/L, indicating that insufficient glucose levels significantly hinder the decolorization process. This highlights the crucial role of glucose as a readily available carbon and energy source for the bacterial isolates, directly influencing their metabolic activity and, consequently, their ability to decolorize dyes.

Glucose influences the decolorization process at the microbial level in several key ways. Firstly, it serves as a primary carbon and energy source. Bacteria utilize glucose for essential metabolic processes, including growth, maintenance, and reproduction. Adequate glucose availability fuels these processes, providing the energy (ATP) and reducing equivalents (NADH) necessary for the enzymatic reactions involved in dye degradation. These reducing equivalents are particularly important in the reductive cleavage of azo dye bonds, a common mechanism for bacterial decolorization. Glucose acts as a crucial electron donor, promoting microbial growth and activity, which in turn enhances azo bond

reduction and dye decolorization (Keziban, 2019). Secondly, glucose can act as a co-metabolite. In some cases, the presence of glucose might be required for the bacteria to effectively utilize the dye as a secondary carbon source or for the enzymes involved in dye degradation to function optimally. While *Pseudomonas putida* WLY could utilize X-3B as its sole carbon source, its slow growth rate suggests that X-3B alone might not be an easily accessible carbon source. The addition of glucose significantly boosted both its growth and decolorization rate, indicating that glucose likely facilitated the utilization of the dye through co-metabolism or by providing an easily accessible form of carbon. Thirdly, glucose can influence the expression and activity of dye-degrading enzymes. It can stimulate the production of crucial enzymes like azoreductases, which are often involved in the initial steps of azo dye breakdown. Essentially, glucose acts as a metabolic trigger, enhancing the bacteria's overall metabolic machinery, including the specific enzymes needed for dye decolorization.
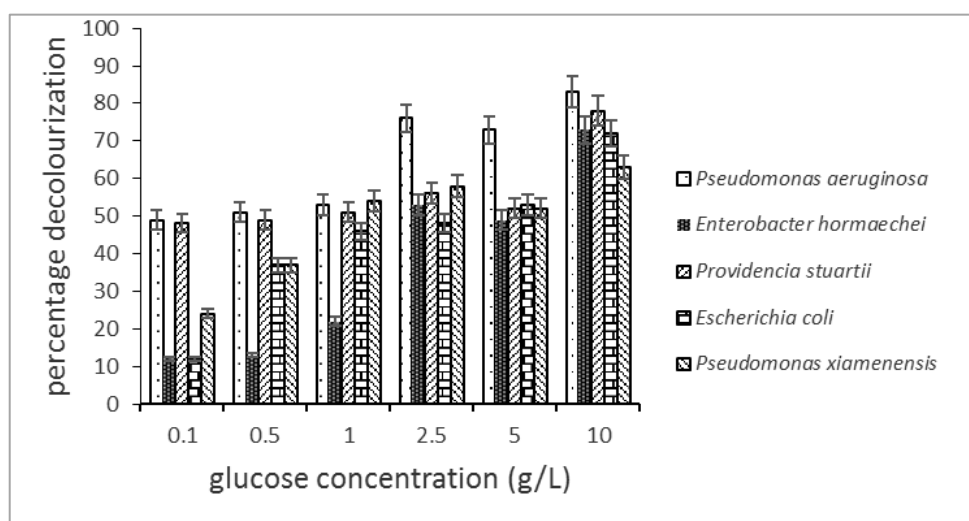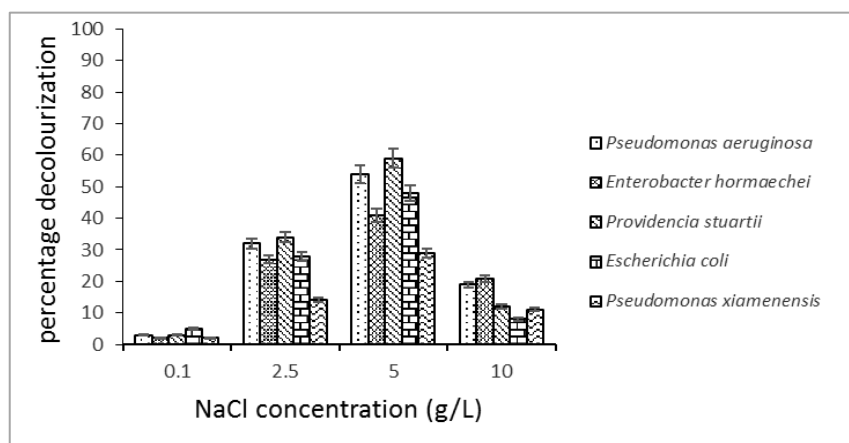

Figure 8. Effect of various glucose concentrations
on decolorization extent of Sudan orange G

The importance of supplementary carbon sources for enhancing bacterial dye decolorization is well-documented. Our finding of 10 g/L glucose as optimal aligns with previous work. For example, Al-Ansari *et al.* (2022) observed improved Acid Orange decolorization by *Enterobacter aerogenes* ES014It with 1.5% glucose (equivalent to 15 g/L), while Sarkar *et al.* (2021) reported enhanced Congo Red removal by *Chryseobacterium geocarposphaerae* DD3 with 5 g/L glucose. Glucose's effectiveness is further supported by Kumaravel and Shanmugam (2024).

While glucose is often preferred, other carbon sources can also play a role. Zhang *et al*. (2021), for instance, showed that fructose co-metabolism enhanced Reactive Black 5 wastewater remediation by a *Pseudomonas aeruginosa* strain. This study reinforces the need to optimize carbon source availability for efficient bioremediation.

The effects of sodium chloride on dye decolorization by various bacterial isolates are detailed in (Figure 9). Optimal decolorization occurred at 5 g/L NaCl, suggesting this concentration promotes optimal microbial activity and efficiency. This aligns with studies suggesting that moderate salinity concentrations, around 5 g/L, are generally optimal for promoting microbial growth and enzyme activity (Hague *et al*., 2023). Tian *et al*. (2021) highlighted the importance of salinity control for effective dye degradation, as it influences microbial activity. Conversely, lower salt levels (0.1 g/L) significantly hindered decolorization. This indicates that while some salt is beneficial, too little can limit the bacteria's metabolic processes necessary for dye breakdown. Sodium chloride, at appropriate concentrations, can contribute to maintaining optimal osmotic pressure for bacterial cells, supporting enzyme activity and nutrient uptake. It can also influence the solubility and availability of the dye itself. However, excessively low salt concentrations can disrupt osmotic balance, potentially hindering cell growth and enzyme function. Our findings also align with Trivedi *et al.* (2022), who observed that Methyl Orange decolorization was unaffected by salinity up to 10 g/L NaCl, with an optimum between 5 and 8 g/L, further supporting the idea of an optimal range. While our study suggests 5 g/L as optimal, the difference may be due to the specific dye, bacterial isolates, or other experimental conditions.

Figure 9. Effect of various sodium chloride concentrations
on the decolorization extent of Sudan orange G

The halotolerance of the isolates, demonstrated by their ability to function in moderate salinity, makes them particularly promising for bioremediation in environments like textile wastewater, which often contains significant amounts of salt.

The impact of sodium citrate on dye decolorization is presented in (Figure 10). Optimal decolorization occurred at 5 g/L, while 10 g/L generally resulted in lower performance, particularly for *E. coli*. Sodium citrate, as a carbon source, can influence the metabolic pathways related to dye degradation. Citrate can be metabolized to provide energy and reducing equivalents, which are essential for the enzymatic breakdown of dyes. However, high concentrations might lead to substrate inhibition or competition for metabolic resources, thus hindering the decolorization process. This may be due to the phenomenon of catabolite repression, wherein the presence of a preferred carbon source (citrate) inhibits the expression of genes required for utilizing the dye. Our optimal concentration of 5 g/L suggests this is an effective concentration, where it promotes bacterial activity but not to an inhibitory extent. Georgiou *et al*. (2004) found that sodium salts can selectively promote the growth of bacteria with high azoreductase activity, which aligns with the observation of improved decolorization. Our results further emphasize the importance of optimizing sodium citrate concentrations, as both insufficient and excessive amounts can negatively impact dye removal.
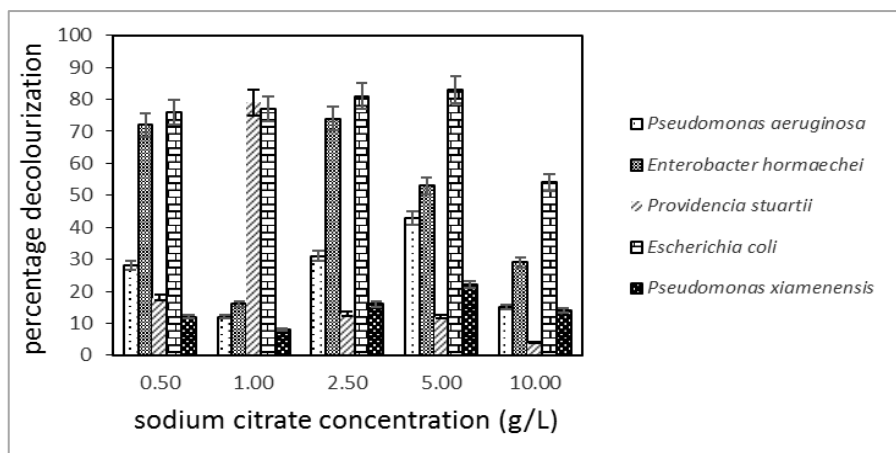
Figure 10. Effect of various sodium citrate concentrations on Sudan orange G

Data on effect of urea on dye decolorization are presented in (Figure 11). A concentration of 0.1 g/L proved optimal, whereas 8 g/L significantly reduced decolorization. Urea serves as a nitrogen source, which is crucial for bacterial

growth and protein synthesis, including the production of dye-degrading enzymes. However, excessively high urea concentrations could lead to ammonia toxicity, inhibiting bacterial growth and activity. High concentrations of urea may increase the pH of the environment, creating unfavorable conditions for the bacteria or the enzymes responsible for dye degradation, or both.
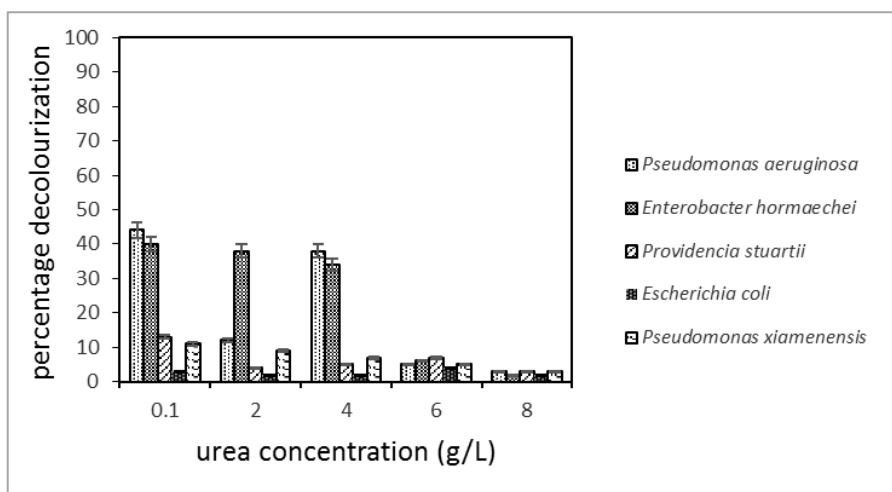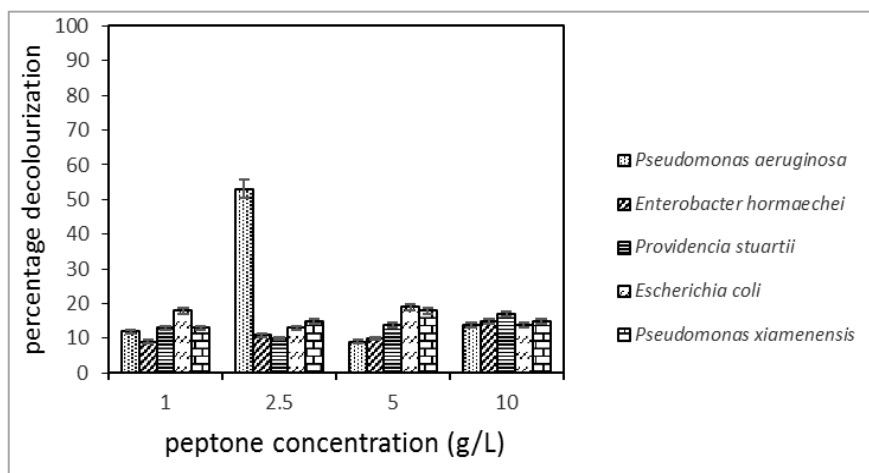

Figure 11. Effect of various urea concentrations
on the decolorization extent of Sudan orange G

Fahad *et al*. (2020) reported that urea, as a nitrogen source, enhances microbial growth and activity, particularly in nitrogen-limited environments, which supports the concept that an optimized amount can be beneficial. Our findings demonstrate that the ideal urea level is low (0.1g/L), which suggests that only a minimal amount is necessary to support nitrogen requirements for efficient dye decolorization and that an excess might have the aforementioned inhibitory effects.

The data obtained on the effect of various peptone concentrations on dye decolorization by bacterial isolates are presented in (Figure 12). Generally, results indicate that there were no significant changes in the extent of decolorization of the azo dyes at different peptone concentrations. This suggests that peptone, a common nitrogen source, may not significantly influence the decolorization efficiency of these bacterial isolates under the conditions tested. Understanding the limited impact of peptone on decolorization is crucial for optimizing nutrient supplementation strategies in bioremediation processes.

Figure 12. Effect of various peptone concentrations
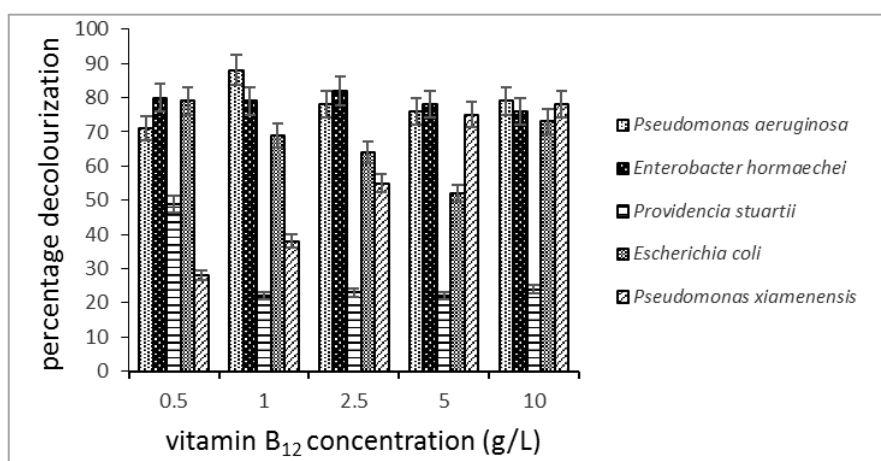on decolorization extent of Sudan orange G.

The effect of vitamin B_2 on dye decolorization by various bacterial isolates is shown in (Figure 13). The data indicate that the optimal decolorization of the dyes was achieved at a vitamin B_2 concentration of 10 g/L. Conversely, the lowest decolorization performance was observed at a concentration of 0.5 g/L.
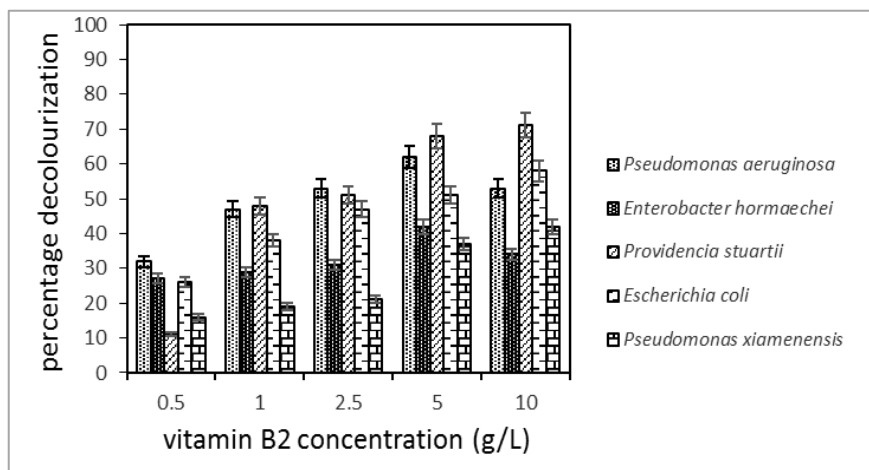
Figure 13. Effect of various vitamin B_2 concentrations
on the decolorization extent of Sudan orange G

These findings highlight the importance of vitamin B_2 in enhancing microbial dye decolorization, potentially due to its role as a coenzyme in various biochemical reactions. Vitamin B_2 can selectively promote the growth of certain microbial populations that are more efficient in dye decolorization. This can lead to a more robust and efficient microbial community capable of higher decolorization rates. Sihang *et al.* (2013) in his study found that the addition of vitamin B_2 enriched specific microbial communities that were more effective at decolorizing textile dyes.

The results on the effects of vitamin B_{12} on dye decolorization by various bacterial isolates is presented in (Figure 14). This paper identified 0.5 mg/L as an optimal concentration for maximizing the decolorization efficiency of azo dyes without causing inhibitory effects. vitamin B_{12} likely enhances decolorization by acting as a cofactor in metabolic pathways critical for dye breakdown. vitamin B_{12} can enhance the decolorization process, however, its concentration must be optimized to avoid potential inhibitory effects.

Figure 14. Effect of various vitamin B_{12} concentrations
on the decolorization extent of Sudan orange G

Interactive effects of multiple variables on the percentage decolorization and microbial growth were investigated using 3-D surface plots (Figure 15), generated by varying two independent variables while holding others at their central levels. This approach, employing response surface methodology, allows visualization of the combined effects of the tested parameters. RSM typically involves statistically designed experiments to assess the influence of multiple factors and their interactions (Table 4). The data are then used to create response surfaces, which depict the relationship between the factors and the measured response (in this case, decolorization and microbial growth). This

allows for optimization of the process by identifying the factor combinations that yield the best results. RSM analysis identified the following ranges as having the greatest impact on both decolorization and microbial growth: pH 6.5-7, temperature 30-35°C, glucose 0.75-1 g/L, and salinity 4.5-5 g/L.
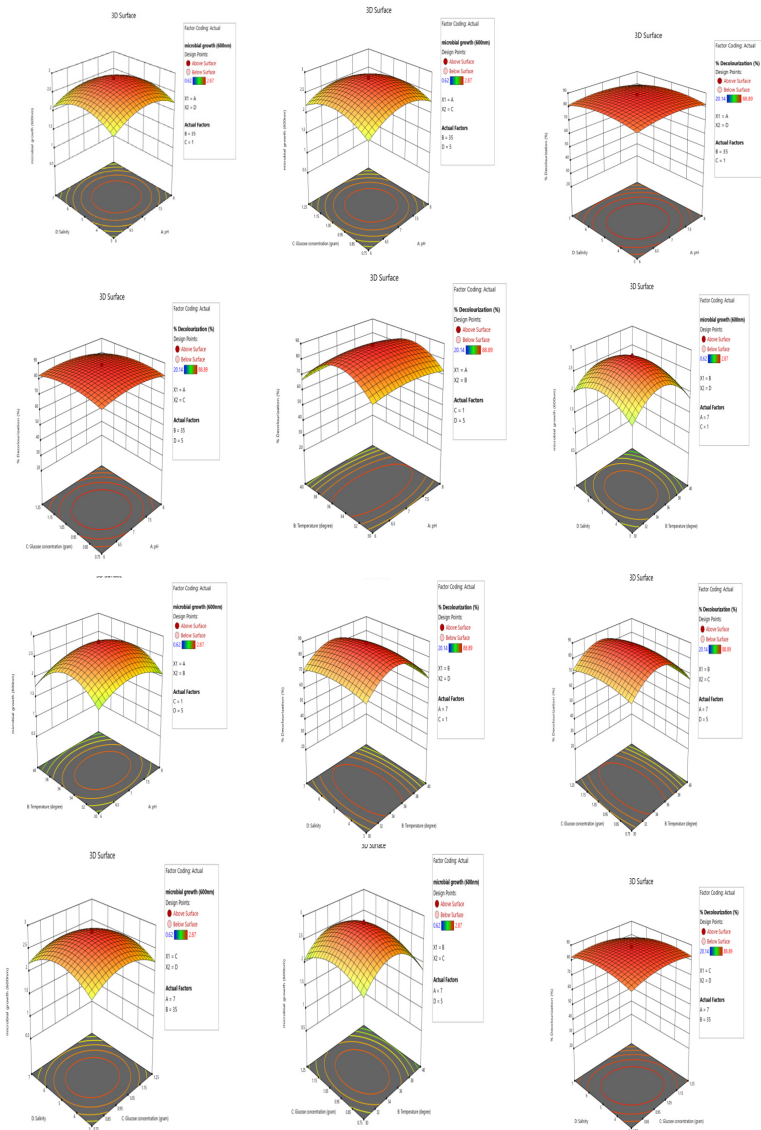

Figure 15. 3-D surface plot for the optimization of Sudan orange G decolorization by isolates in consortium of various parameters

Table 4. Composition of various experiments of the CCD for independent variables and responses (actual and predicted) by isolates in Consortium in Sudan orange G

| Run	A; pH	B: Temp (t)	C: Glucose Conc. (g)	D: Salinity (g)	% Decolorization		Microbial Growth (600 nm)	
					Actual	Predicted	Actual	Predicted
1	5	35	1	5	73.45	76.58	1.52	1.50
2	6	30	0.75	3	66.81	64.97	1.38	1.37
3	8	40	1.25	7	53.07	52.88	0.96	0.99
4	8	30	0.75	7	68.98	67.33	1.48	1.51
5	8	40	0.75	7	58.45	59.15	0.98	1.20
6	8	30	0.75	3	65.14	66.01	1.38	1.50
7	8	30	1.25	7	63.89	62.02	1.32	1.32
8	7	35	1	1	75.78	75.16	1.68	1.54
9	6	30	1.25	7	66.82	65.07	1.42	1.42
10	7	35	1	9	67.88	71.26	1.44	1.36
11	8	40	1.25	3	58.78	59.37	0.97	1.22
12	7	35	1.5	5	70.75	72.78	1.58	1.56
13	6	40	0.75	7	62.14	60.30	0.99	1.22
14	6	30	1.25	3	69.84	68.41	1.49	1.46
15	7	45	1	5	20.14	19.69	0.62	0.30
16	7	35	1	5	87.81	88.25	2.78	2.82
17	9	35	1	5	74.01	73.64	1.78	1.58
18	7	35	1	5	88.04	88.25	2.81	2.82
19	7	25	1	5	31.01	34.22	0.72	0.83
20	6	30	0.75	7	68.89	67.57	1.47	1.41
21	6	40	1.25	7	58.45	56.85	0.98	1.05
22	6	40	1.25	3	62.45	62.07	1.24	1.24
23	7	35	1	5	88.89	88.25	2.87	2.82
24	8	30	1.25	3	66.81	66.62	1.48	1.42
25	7	35	0.5	5	74.89	75.62	1.87	1.67
26	6	40	0.75	3	58.45	59.59	0.98	1.17
27	8	40	0.75	3	59.98	59.70	1.31	1.34

Data obtained on power generation (Figure 16) show that the microbial consortium in the microbial fuel cell (MFC) generated 127 mV and achieved 90% decolorization of Sudan orange G within 24 hours. Following this peak, the electric power generation gradually declined. This demonstrates the potential of MFCs to effectively degrade dyes while simultaneously generating electricity, offering a sustainable, dual-benefit bioremediation approach. Optimizing MFC operating conditions can further enhance both decolorization efficiency and power generation, making this technology promising for environmental management. The observed correlation between power generation and dye decolorization suggests a direct link between microbial activity and electron release. As the bacteria degrade the dye, they release electrons, which contribute

to the increased power output. Microbial redox reactions release electrons, which are transferred to the MFC anode, generating a current. Efficient dye decolorization fuels electron release and thus power generation. However, as the dye substrate is depleted, electron release and power generation may decline. This dynamic interplay between power generation and dye decolorization in MFCs has been observed and studied by others, as highlighted by Li *et al.* (2021).
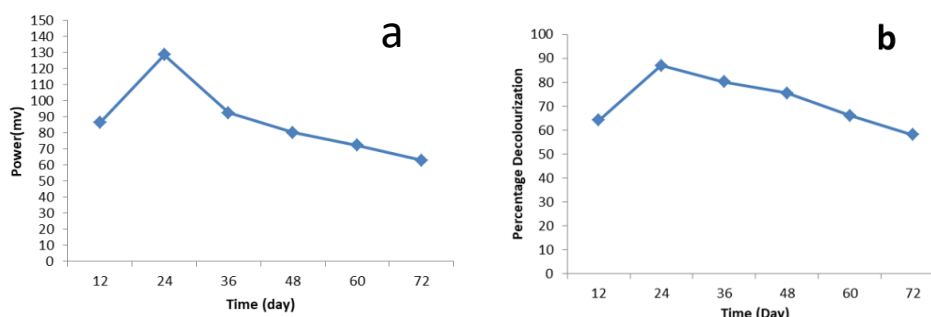

Figure 16. Changes in average daily power (**a**) generated with time and decolourization (**b**) of Sudan orange G by bacterial consortium coupled to MFC during bioremediation study

The GC-MS chromatograms (Figures 17-19) provide strong evidence of the azo dye's transformation after optimization and MFC treatment. The emergence of various degradation metabolites demonstrates the comprehensive breakdown of the dye into simpler compounds. Specifically, the identified metabolites post-MFC treatment were undecanoic acid, 10-methyl-, methyl ester, cyclopentane, and cyclopropylidene-2(1H)-naphthalenone. Undecanoic acid, 10-methyl-, methyl ester, a branched fatty acid ester, suggests bacterial utilization of dye components as carbon/energy sources. Cyclopentane, a simple alkane, indicates the breakdown of aromatic structures into smaller aliphatic components. Cyclopropylidene-2(1H)-naphthalenone, a cyclic ketone with a modified naphthalene ring, likely represents a degradation intermediate, suggesting further transformation is ongoing. These metabolites demonstrate the consortium's ability to degrade the dye into less complex, potentially less toxic compounds. This clearly illustrates the bacterial consortium's ability to not only decolorize but also effectively degrade the azo dye into potentially less harmful substances. This transformation highlights the efficacy of MFC technology for treating environmental contaminants and advancing sustainable wastewater treatment.
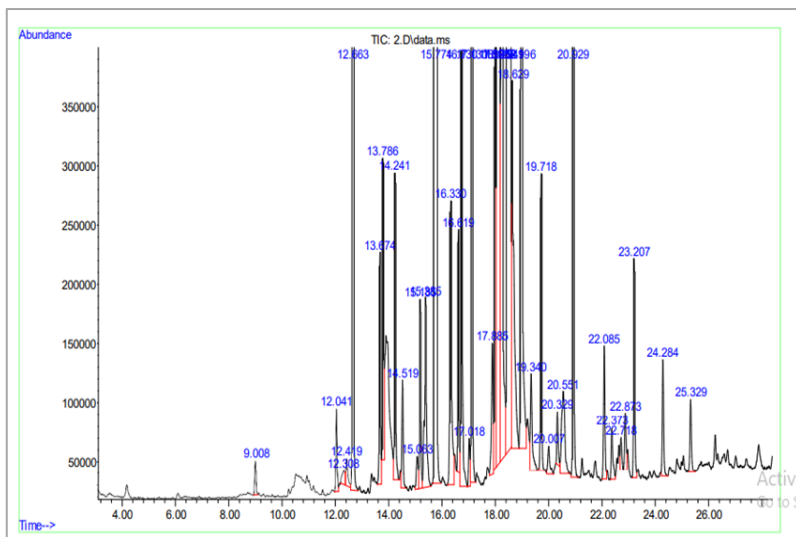
Figure 17. GC-MS chromatogram of the synthetic dye wastewater containing Sudan orange G before decolorization by bacterial consortium**.**
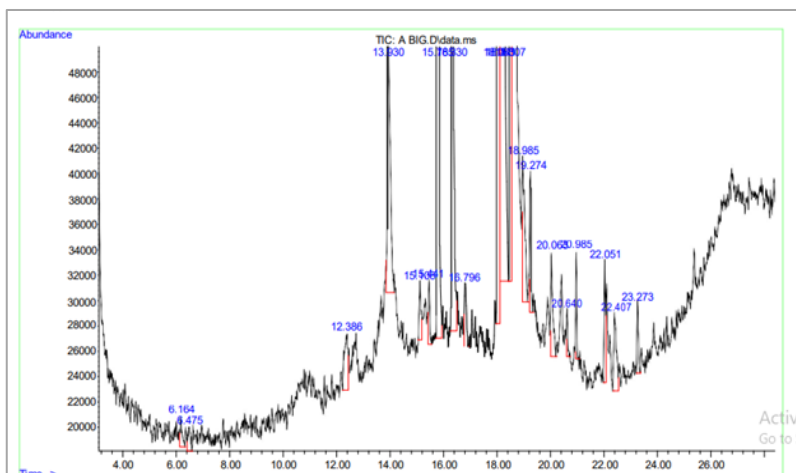
Figure 18. GC-MS chromatogram of decolorized Sudan orange G indicating degradation fractions after optimization of dye decolorization by bacterial consortium using RSM.
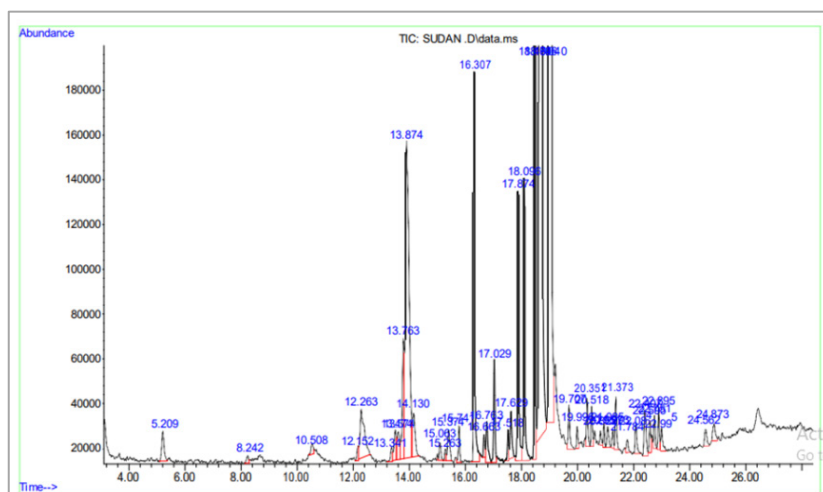
Figure 19. GC-MS chromatogram of decolorized Sudan orange G indicating degradation fractions after dye decolorization by bacterial consortium in the MFC.

Conclusion

The comprehensive dataset derived from this study substantiates the efficacy of *Pseudomonas aeruginosa* (MW584979), *Enterobacter hormaechei* (MW584986), *Providencia stuartii* (MW584987), *Escherichia coli* (MZ394117), and *Pseudomonas xiamenensis* (MW585052) in the degradation of azo dyes, particularly Sudan orange G. Notably, *Pseudomonas aeruginosa* (MW584979) and *Providencia stuartii* (MW584987) were found to harbor the azoreductase gene, further corroborating their ability to catalyze dye degradation processes. The utilization of a consortium approach, facilitated by response surface methodology, emerged as an effective strategy for optimizing culture conditions, as initially obtained through the One Factor at a Time (OFAT) method. This methodological synergy allowed for the maximization of dye decolorization, with experimental and predicted values demonstrating the practical utility of RSM. Remarkably, the manipulation of process variables resulted in a substantial enhancement of dye decolorization, reaching up to 88% within 24 hours. Furthermore, when integrated into a microbial fuel cell setup, this approach yielded a remarkable 92% decolorization efficiency alongside a notable power output of 130 mV. The metabolites produced during this process were further analyzed through GC-MS chromatography, revealing not only dye decolorization but also significant degradation, thereby underscoring the multifaceted remediation capabilities of

115

the microbial culture under investigation. Enhancing Sudan G decolorization and electricity generation in a dual-chambered MFC not only addresses the environmental issue of dye pollution but also contributes to sustainable energy production. Optimizing microbial activity, electrode materials, and operating conditions integrates environmental remediation with renewable energy generation, paving the way for practical applications of MFCs in wastewater treatment and energy production.

Conflict of Interest

The authors declare that they have no known competing financial interests or personal relationships that could have appeared to influence the work reported in this manuscript.

Authors' Contributions

Conceptualization and methodology were led by Prof. C.J. Ogugbue. Investigation and data curation were conducted by Mr. C.J. Echejiuba and Dr. I.S. Obuekwe. Supervision was provided by Prof. C.J. Ogugbue**.** Funding acquisition was secured by Mr. C.J Echejiuba. All authors have read and approved the final version of the manuscript for publication.

References

Al-Ansari, M.M., Li, Z., Masood, A. & Rajaselvam, J. (2022). Decolourization of azo dye using a batch bioreactor by an indigenous bacterium *Enterobacter aerogenes* ES014 from the waste water dye effluent and toxicity analysis. *Environ Res, 205*, 112189. https://doi.org/10.1016/j.envres.2021.112189

Al-Tohamy, R., Ali S. S., Xie, R., Schager, M., Khalil, M. A. & Sun, J. (2023). Decolorization of reactive azo dye using novel halotolerant yeast consortium HYC and proposed degradation pathway. *Ecotoxicol Environ Safe, 263,* 115258. https://doi.org/10.1016/j.ecoenv.2023.115258

Cao, J., Sanganyado, E., Liu, W., Zhang, W. & Liu, Y. (2019). Decolorization and detoxification of Direct Blue 2B by indigenous bacterial consortium. *J Environ Manage, 242,* 229-237. https://doi.org/10.1016/j.jenvman.2019.04.067

Chen, G., An, X., Li, H., Lai, F., Yuan, E., Xia, X. & Zhang, Q. (2021). Detoxification of azo dye Direct Black G by thermophilic *Anoxybacillus* sp. PDR2 and its application potential in bioremediation. *Ecotoxicol Environ Safe, 214,* 112084. https://doi.org/10.1016/j.ecoenv.2021.112084

Chen, K., Wua, J., Liou, D. H. & Sz-Chwun, J. (2003). Decolorization of the textile dyes by newly isolated bacterial strains. *J Biotechnol, 101*, 57–68. https://doi.org/10.1016/s0168-1656(02)00303-6

Dafale, N., Wate, S., Meshram, S. & Nandy, T. (2008). Kinetic study approach of 117emazol black-B use for the development of two-stage anoxic–oxic reactor for decolorization/biodegradation of azo dyes by activated bacterial consortium. *J Hazard Mater*, *159*(2-3), 319–328. https://doi.org/10.1016/j.jhazmat.2008.02.058

Das, A. & Mishra, S. (2017). Removal of textile dye reactive green-19 using bacterial consortium: Process optimization using response surface methodology and kinetics study. *J Environ Chem Eng*, *5*(1), 612-627. https://doi.org/10.1016/j.jece.2016.10.005

Eslami, M., Amoozegar, M. A. & Asad, S. (2016). Isolation, cloning and characterization of an azoreductase from the halophilic bacterium *Halomonas elongata*. *Int. J. Biol. Macromol.*, *85*, 111–116.

Etezad, S. M., & Sadeghi-Kiakhani, M. (2021). Decolorization of malachite green dye solution by bacterial biodegradation. *Prog. Color Colorants Coat.*, *14*(2), 79-87.

Fahad, A. A., Abdulaziz, A.A., Hamdah, S.A., Amjad, A.A. & Naushad, A., (2020). Photocatalytic blue and rose bengal by using urea derived g-C$_3$N$_4$/ZnO nanocomposites. *Innov Catalytic Photocatalytic Systems Environ Remediation*, *10* (12), 1457. https://doi.org/10.3390/catal10121457

Felsenstein, J. (1985). Phylogenies and the comparative method. *Am. Nat, 125*(1),1–15. https://doi.org/10.1111/j.1558-5646.1985.tb00420.x

Firoozeh, F., Shahamat, Y. D., Rodríguez-Couto, S., Kouhsari, E. & Farhad, N. F. (2022). Bioremediation for the decolorization of textile dyes by bacterial strains isolated from dyeing wastewater. *Jordan J Biol Sci, 15*(2), 219-225. https://doi.org/10.54319/jjbs/150209

Georgiou, D., Metallinou, C., Aivasidis, A., Voudrias, E. & Gimouhopoulos, K. (2004). Decolorization of azo-reactive dyes and cotton-textile wastewater using anaerobic digestion and acetate-consuming bacteria. *Biochem Eng J*, *19*(1), 75–79. https://doi.org/10.1016/j.bej.2003.11.003

Gul, H., Raza, W., Lee, J., Azam, M., Ashraf, M. & Kim, K. (2021). Progress in microbial fuel cell technology for wastewater treatment and energy harvesting. *Chemosphere, 281*, 130828. https://doi.org/10.1016/j.chemosphere.2021.130828

Hague, M.M., Hague, M.K., Mosharaf, M.K., Rahman, A.,Islam, M.S., Nahar, K. & Molla, A.H. (2023). Enhanced biofilm-mediated degradation of carcinogenic and mutagenic azo dye by novel bacteria isolated from tannery wastewater. *J Environ Chem Eng, 11*(42), 110731. https://doi.org/10.1016/j.jece.2023.110731

Hu, L, Liu, N., Li, C., Mao, J., Li, M., Yun, Y. & Liu, W. (2023). Performance and response of coupled microbial fuel cells for enhanced anaerobic treatment of azo dye wastewater with simultaneous recovery of electrical energy. *Environ Sci Pollut Res Int, 30*(38), 89495-89509. https://doi.org/10.1007/s11356-023-28582-x

Ikram, M., Naeem, M., Zahoor, M., Hanafiah, M. M., Oyekanmi, A. A., Islam, N. U. & Sadiq, A. (2022). *Bacillus subtilis*: As an efficient bacterial strain for the reclamation of water loaded with textile azo dye, orange II. *Int J Mol Sci*, *23*(18), 10637.

Jukes, T.H. & Cantor, C.R. (1969). Evolution of protein molecules: Mammalian protein metabolism. *Academic Press, New York*, 21-132. http://dx.doi.org/10.1016/B978-1-4832-3211-9.50009-7

Kapdan, I.K., Kargi,F., McMullan, G. & Marchant, R. (2000). Decolorization of textile dyestuffs by a mixed bacterial consortium. *Biotechnol Lett, 22*, 1191181. http://dx.doi.org/10.1023/A:1005641430613

Keziban, A., Nuray, G., Soner, C. & Mahmut, O. (2019). Efficiency of glucose oxidase immobilized on tannin modified $NiFe_2O_4$ nanoparticles on decolorization of dye in the fenton and photo-biocatalyic processes. *J Photochem Photobiol*, *382,* 111935. https://doi.org/10.1016/j.jphotochem.2019.111935

Kumaravel, R. & Shanmugam, V. K. (2024). Biomimetic and ecological perspective towards decolorization of industrial important Azo dyes using bacterial cultures–A review. *Sustainable Chemistry for the Environment*, p. 100130. https://doi.org/10.1016/j.scenv.2024.100130

Ilamathi, R. & Jayapriya, J. (2017). Microbial fuel cells for dye decolorization. *Environ Chem Lett, 16,* 239-250 https://doi.org/10.1007/s10311-017-0669-4

Li, T., Song, H. L., Xu, H., Yang, X. L. & Chen, Q. L. (2021). Biological detoxification and decolorization enhancement of azo dye by introducing natural electron mediators in MFCs. *J Hazard Mater*, *416,* 125864. https://doi.org/10.1016/j.jhazmat.2021.125864

Liu, W., Liu, L., Liu, C., Hao, Y., Yang, H., Yuan, B. & Jiang, J. (2016). Methylene blue enhances the anaerobic decolorization and detoxication of azo dye by *Shewanella onediensis* MR-1. *Biochem Eng J*, *110*, 115–124. https://doi.org/10.1016/j.bej.2016.02.012

Liu, Y., Huang, L., Guo, W., Jia, L., Fu, Y., Gui, S. & Lu, F. (2017). Cloning, expression, and characterization of a thermostable and pH-stable laccase from *Klebsiella pneumoniae* and its application to dye decolorization. *Process Biochem*, *53,* 125– 134. https://doi.org/10.1016/j.procbio.2016.11.015

Madhushika, H. G., Ariyadasa, T. U. & Gunawardena, S. H. P. (2021). Biodegradation of reactive yellow EXF dye: optimization of physiochemical parameters and analysis of degradation products. *Int J Environ Sci Technol*, 1-12.

Matteo, D., Anna, E. T., Barbara, L., Pierangela, C., Maddalena, P., Elham, J., Giuseppina, B. & Andrea, F. (2018). Bioelectrochemical BTEX removal at different voltages: assessment of the degradation and characterization of the microbial communities. *J Hazard Mater, 341*, 120-127. https://doi.org/10.1016/j.jhazmat.2017.07.054

Mendes, S., Pereira, L., Batista, C., & Martins, L. O. (2011). Molecular determinants of azo reduction activity in the strain *Pseudomonas putida* MET94. *Appl Microbiol Biotechnol*, *92*(2), 393–405.

Mittal, N. & Kumar, A. (2022). Microbial fuel cell as water-energy environment nexus: a relevant strategy for treating streamlined effluents. *Energy Nexus, 7*, 100097. https://doi.org/10.1016/j.nexus.2022.100097

Md Burhan Kabir Suhan, S.M. Tanveer Mahtab, Wafi Aziz, Sonia Akter, & Md Shahinoor Islam (2021). Sudan black B dye degradation in aqueous solution by fenton oxidation process: kinetics and cost analysis. *Case Stud Chem Environ Eng, 4,* 100126. https://doi.org/10.1016/j.cscee.2021.10012

Mugerfeld, I., Law, B. A., Wickham, G. S. & Thompson, D. K. (2009). A putative azoreductase gene is involved in the *Shewanella oneidensis* response to heavy metal stress. *Appl Microbiol Biotechnol*, *82*(6), 1131–1141.

Ngo, A. C. R. & Tischler, D. (2022). Microbial degradation of azo dyes: approaches and prospects for a hazard-free conversion by microorganisms. *J Environ Sci Pub Health*, *19*, 4740. https://doi.org/10.3390/ijerph19084740

NIST (2008). Glucose in Frozen Human Serum. National Institute of Standards & Technology Certificate of Analysis, In: Linstrom PJ, Mallard WG (eds). NIST Chemistry WebBook. NIST Standard Reference Database Number 965a. Gaithersburg, MD 20899 *National Institute of Standards and Technology*, 2011, 20899, http://webbook.nist.gov (retrieved April 27, 2011)

Nk, S. & Rahman, R. (2020). Microbial fuel cell an alternative for treatment of textile wastewater. *Int Res J Eng Technol*, *7*(4), 3962-3967.

OECD (2017), OECD Due Diligence Guidance for Responsible Supply Chains in the Garment and Footwear Sector, OECD Publishing, Paris. https://doi.org/10.1787/9789264290587-en

Qi, J., Paul, C. E., Hollmann, F. & Tischler, D. (2017). Changing the electron donor improves azoreductase dye degrading activity at neutral pH. *Enzyme Microb Technol*, *100*, 17–19.

Qi, J., Schlömann, M. & Tischler, D. (2016). Biochemical characterization of an azoreductase from *Rhodococcus opacus* 1CP possessing methyl red degradation ability. *Journal of Molecular Catalysis B: Enzymatic*, *130*, 9–17.

Rafaqat, S., Ali, N. Torres, C., C. & Rittmann, B. (2022). Recent progress in treatment of dyes wastewater using microbial-electro-Fenton technology. *RSC Advances*, *12,* 17104-17137. https://doi.org/10.1039/D2RA01831D

Sarkar, S., Echeverría-Vega, A., Banerjee, A. & Bandopadhyay, R. (2021). decolorisation and biodegradation of textile di-azo dye Congo red by chryseobacterium geocarposphaerae DD3. *Sustainability*, *13*(19), 10850.

Sihang, S, Pengfei, F. Yi, X. & Geng, Q. (2013). Experimental research of decoloring treatment on vitamin B_{12} wasterwater. *Appl Mech Mater, 295*-298:1209-1214 http://dx.doi.org/10.4028/www.scientific. net/AMM.295-298.1209

Sikder, S. & Rahman, M. M. (2023). Efficiency of microbial fuel cell in wastewater (municipal, textile and tannery) treatment and bioelectricity production. *Case Stud Chem Environ Eng, 8,* 100421. https://doi.org/10.1016/j.cscee.2023.100421

Saitou, N. & Nei, M. (1987). The neighbor-joining method: a new method for reconstructing phylogenetic trees. *Mol Biol Evol, 4*(4), 406-25. https://doi.org/ 10.1093/oxfordjournals.molbev.a040454. PMID: 3447015.

Taha, M., Adetutu, E.M., Shahsavari, E., Smith, A.t. & Ball, A.S., (2014). Azo and anthraquinone dye mixture decolorization at elevated temperature and concentration by a newly isolated thermophilic fungus, *Thermomucor indicae-seudaticae. J Environ Chem Eng, 2*(1), 415-423. https://doi.org/10.1016/j.jece.2014.01.015

Tahir, U., Nawaz, S., Hassan Khan, U. & Yasmin, A. (2021). Assessment of biodecolorization potentials of biofilm forming bacteria from two different genera for mordant black 11 dye. *Bioremediation Journal*, *25*(3), 252-270.

Tian, F., Wang, Y., Guo, G., Ding, K., Yang, F., Wang, H. & Liu, C. (2021). Enhanced azo dye biodegradation at high salinity by a halophilic bacterial consortium. *Bioresource Technol.*, *326*, 124749.
https://doi.org10.1016/j.biortech.2021.124749

Trivedi, A., Desireddy, S. & Chacko, S.P. (2022). Effect of pH, salinity, dye, and biomass concentration on decolorization of azo dye methyl orange in denitrifying conditions. *Water, 14,* 3747. https://doi.org/10.3390/w14223747

Umar, A., Abid, I., Antar, M., Dufossé, L., Hajji-Hedf, L., Elshikh, M. S., Abeer El Shahawy, A. & Abdel-Azeem, A. M. (2023). Electricity generation and oxidoreductase potential during dye discoloration by laccase-producing *Ganoderma gibbosum* in fungal fuel cell. *Microb cell fact, 22*, 258. https://doi.org/10.1186/s12934-023-02258-0

Uppala, R., Sundar, K. & Muthukumaran, A. (2015). Response surface methodology mediated optimization of decolorization of azo dye amido black 10B by *Kocuria kristinae* RC3. *Inter J Environ Sci Technol*, 2018, 1–12.
https://doi.org/10.1007/s13762-018-1888-3

Zhang, Q., Xie, X., Xu, D., Hong, R., Wu, J., Zeng, X. & Liu, J. (2021). Accelerated azo dye biodegradation and detoxification by *Pseudomonas aeruginosa* DDMZ1-2 via fructose co-metabolism. *Environ Technol Innov*, *24*, 101878.